PROCEEDINGS OF SPIE

SPIEDigitalLibrary.org/conference-proceedings-of-spie

Measuring 3D molecular orientation and rotational mobility using a Trispot point spread function

Oumeng Zhang, Tianben Ding, Jin Lu, Hesam Mazidi, Matthew D. Lew

Oumeng Zhang, Tianben Ding, Jin Lu, Hesam Mazidi, Matthew D. Lew, "Measuring 3D molecular orientation and rotational mobility using a Tri-spot point spread function," Proc. SPIE 10500, Single Molecule Spectroscopy and Superresolution Imaging XI, 105000B (20 February 2018); doi: 10.1117/12.2287004



Event: SPIE BiOS, 2018, San Francisco, California, United States

Measuring 3D molecular orientation and rotational mobility using a Tri-spot point spread function

Oumeng Zhang^a, Tianben Ding^a, Jin Lu^a, Hesam Mazidi^a, Matthew D. Lew*^a
^aDepartment of Electrical and Systems Engineering, Washington University in St. Louis,

1 Brookings Drive, St. Louis, MO, USA 63130

ABSTRACT

We present a method to measure the molecular orientation and rotational mobility of single-molecule emitters by designing and implementing a Tri-spot point spread function. It can measure all degrees of freedom related to molecular orientation and rotational mobility. Its design is optimized by maximizing the theoretical limit of its measurement precision. We evaluate the precision and accuracy of the Tri-spot PSF by measuring the orientation and effective rotational mobility of single fluorescent molecules embedded in a polymer matrix.

Keywords: single-molecule imaging, fluorescence microscopy, point spread function engineering, phase mask design

1. INTRODUCTION

Single-molecule imaging techniques have become invaluable for probing the heterogeneity of both biological and abiological systems with nanoscale resolution. The unique versatility of these nanometer-sized probes stems from their ability to encode interactions with their local environment into the fluorescence that they emit, as evidenced by heterogeneous absorption spectra of single molecules first observed decades ago¹. Recently, these techniques have gained popularity for their capability to produce images of structures within living cells with resolution beyond the Abbé diffraction limit (~250 nm for visible light). Super-resolution optical techiques²⁻⁴ that repeatedly record the position of individual molecules over time to construct super-resolved images are known collectively as single-molecule localization microscopes (SMLM).

Beyond tracking the position and spectra of individual molecules, probing their orientation has provided valuable insight into a number of biological systems⁵, including molecular motors^{6–9}. Molecular orientation can be inferred by measuring a molecule's fluorescence intensity in response to varying polarizations of excitation light¹⁰, measuring its fluorescence intensity in one or more polarized detection channels¹¹, measuring the angular spectrum of its fluorescence emission^{12,13}, or some combination of the aforementioned techniques.

Recently, point spread function (PSF) engineering, or direct design of an optical instrument's impulse response, has been used to great advantage to augment super-resolution microscopes with 3D imaging^{14–18} and even multicolor¹⁹ capabilities. Other techniques, such as the bisected²⁰ and quadrated²¹ pupils and the double-helix²² PSF, have been designed to measure the orientation of individual fluorescent molecules.

Here, we describe an intensity-based image-formation model for our microscope in response to a dipole-like emitter. By examining this model, we design the Tri-spot PSF, which contains the same number of spots as the number of orientational degrees of freedom within the model. The Tri-spot PSF enables the simultaneous measurement of molecular orientation and rotational mobility with high signal-to-background ratio. We evaluate the precision and accuracy of orientation measurements with the Tri-spot PSF via imaging simulations and experimental measurements of fluorescent molecules.

2. TRI-SPOT PSF DESIGN

2.1 Forward imaging model

We model a single fluorescent molecule as an oscillating electric dipole with an orientation parametrized by a unit vector μ given by

*mdlew@wustl.edu; phone 1-314-935-6790; fax 1-314-935-7500; lewlab.wustl.edu

Single Molecule Spectroscopy and Superresolution Imaging XI, edited by Jörg Enderlein, Ingo Gregor, Zygmunt Karol Gryczynski, Rainer Erdmann, Felix Koberling, Proc. of SPIE Vol. 10500, 105000B © 2018 SPIE · CCC code: 1605-7422/18/\$18 · doi: 10.1117/12.2287004

Proc. of SPIE Vol. 10500 105000B-1

$$\mu = \begin{bmatrix} \mu_x \\ \mu_y \\ \mu_z \end{bmatrix} = \begin{bmatrix} \sin \theta \cos \phi \\ \sin \theta \sin \phi \\ \cos \theta \end{bmatrix} \tag{1}$$

where μ_x , μ_y , and μ_z denote the projection of μ onto each Cartesian axis. We can also use the polar angle θ and azimuthal angle ϕ in spherical coordinates to represent this vector. After modeling the propagation of light through the objective lens and tube lens, the intensity distribution of the electric field in the image plane is given by ¹³

$$I_{x(y)} = I_0 \begin{bmatrix} B_{XX,x(y)} \\ B_{YY,x(y)} \\ B_{ZZ,x(y)} \\ B_{XY,x(y)} \\ B_{XZ,x(y)} \\ B_{YZ,x(y)} \end{bmatrix}^T \begin{bmatrix} \mu_x^2 \\ \mu_y^2 \\ \mu_z^2 \\ \mu_x \mu_y \\ \mu_x \mu_z \\ \mu_y \mu_z \end{bmatrix} = I_0 \boldsymbol{B}_{x(y)} \boldsymbol{M}$$
(2)

where I_0 gives the total number of photons captured in the image and $\boldsymbol{B}_{x(y)} = [B_{XX,x(y)}, \dots, B_{YZ,x(y)}]$ are the basis images of the system in response to a dipole emitter whose orientational second moments are given by $\boldsymbol{M} = [\mu_x^2, \dots, \mu_y \mu_z]^T$. The subscripts x(y) refer to x-polarized and y-polarized images, respectively, if a polarizing beamsplitter is used to create two imaging channels²². Note that the basis images are independent of emitter orientation. Therefore, we wish to design the basis images $\boldsymbol{B}_{x(y)}$ to maximize the precision of measuring the orientational second-moments \boldsymbol{M} of a dipole-like emitter.

If the emitter is rotating over time, then the orientational second-moment trajectories can be integrated over the camera's exposure time *T* to model the resulting image:

$$I_{x(y)} = \frac{I_0}{T} \boldsymbol{B}_{x(y)} \begin{bmatrix} \int_0^T \mu_x(t)^2 \, \mathrm{d}t \\ \int_0^T \mu_y(t)^2 \, \mathrm{d}t \\ \int_0^T \mu_z(t)^2 \, \mathrm{d}t \\ \int_0^T \mu_z(t) \mu_y(t) \, \mathrm{d}t \\ \int_0^T \mu_x(t) \mu_z(t) \, \mathrm{d}t \\ \int_0^T \mu_x(t) \mu_z(t) \, \mathrm{d}t \end{bmatrix} = I_0 \boldsymbol{B}_{x(y)} \begin{bmatrix} \langle \mu_x(t)^2 \rangle \\ \langle \mu_y(t)^2 \rangle \\ \langle \mu_z(t)^2 \rangle \\ \langle \mu_z(t)^2 \rangle \\ \langle \mu_x(t) \mu_y(t) \rangle \\ \langle \mu_x(t) \mu_z(t) \rangle \\ \langle \mu_y(t) \mu_z(t) \rangle \end{bmatrix}$$

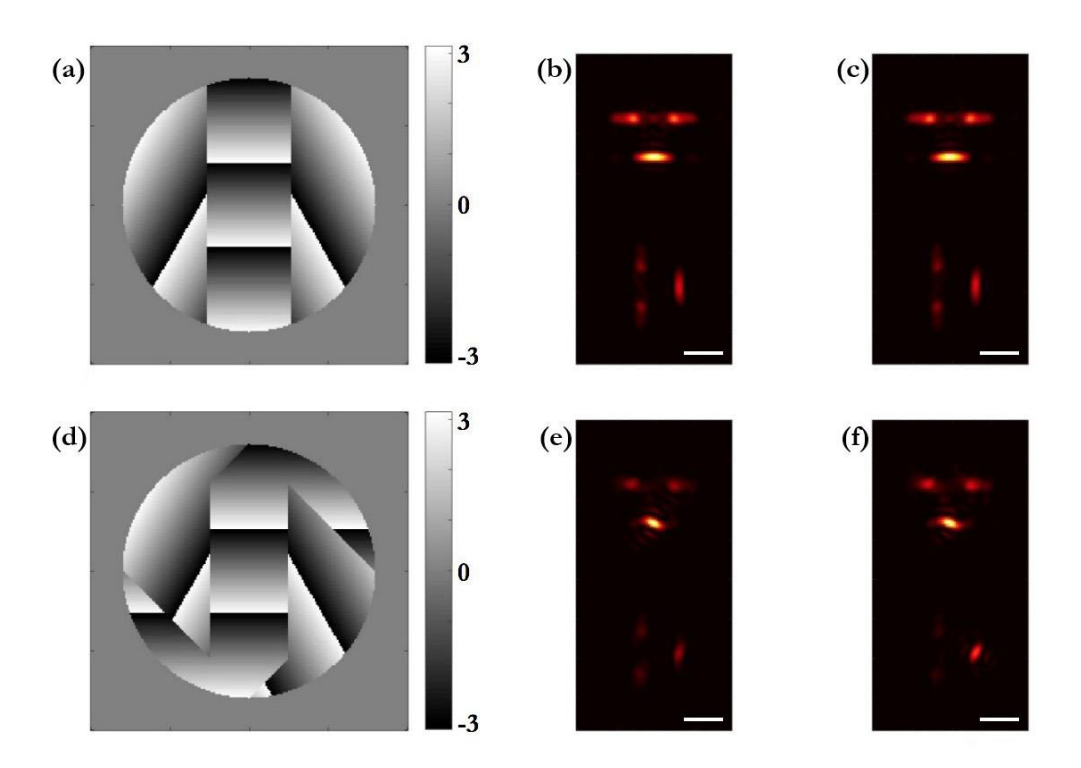
$$(3)$$

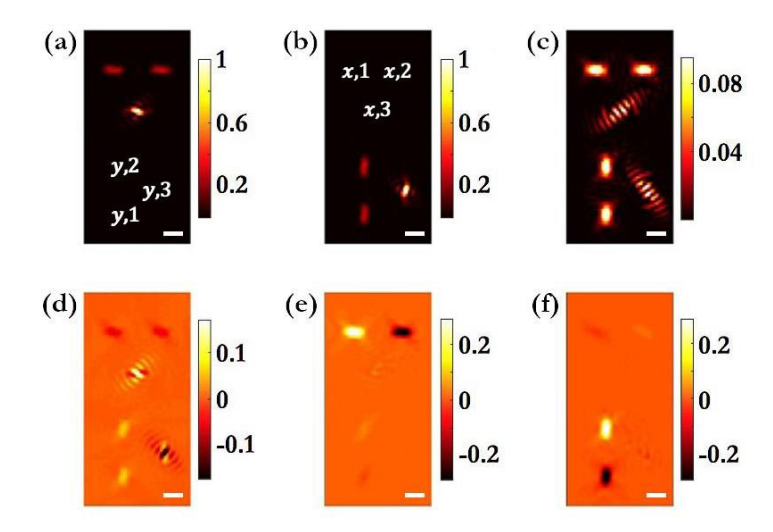
where $\langle \cdot \rangle$ denotes a temporal average. If a nanoscale emitter is composed of several or many independent dipole-like emitters, then the integrals over time in Eq. (3) can be replaced by discrete sums over the ensemble of emitters. For example, an isotropic emitter has second moments $\mathbf{M} = [1/3,1/3,1/3,0,0,0]^T$, while a molecule fixed in orientation $\boldsymbol{\mu}$ has second moments $\mathbf{M} = [\mu_x^2, \mu_y^2, \mu_z^2, \mu_x \mu_y, \mu_x \mu_z, \mu_y \mu_z]^T$.

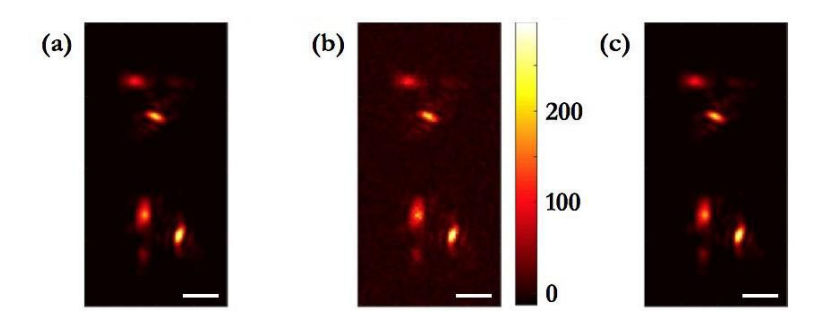
2.2 Designing the Tri-spot PSF

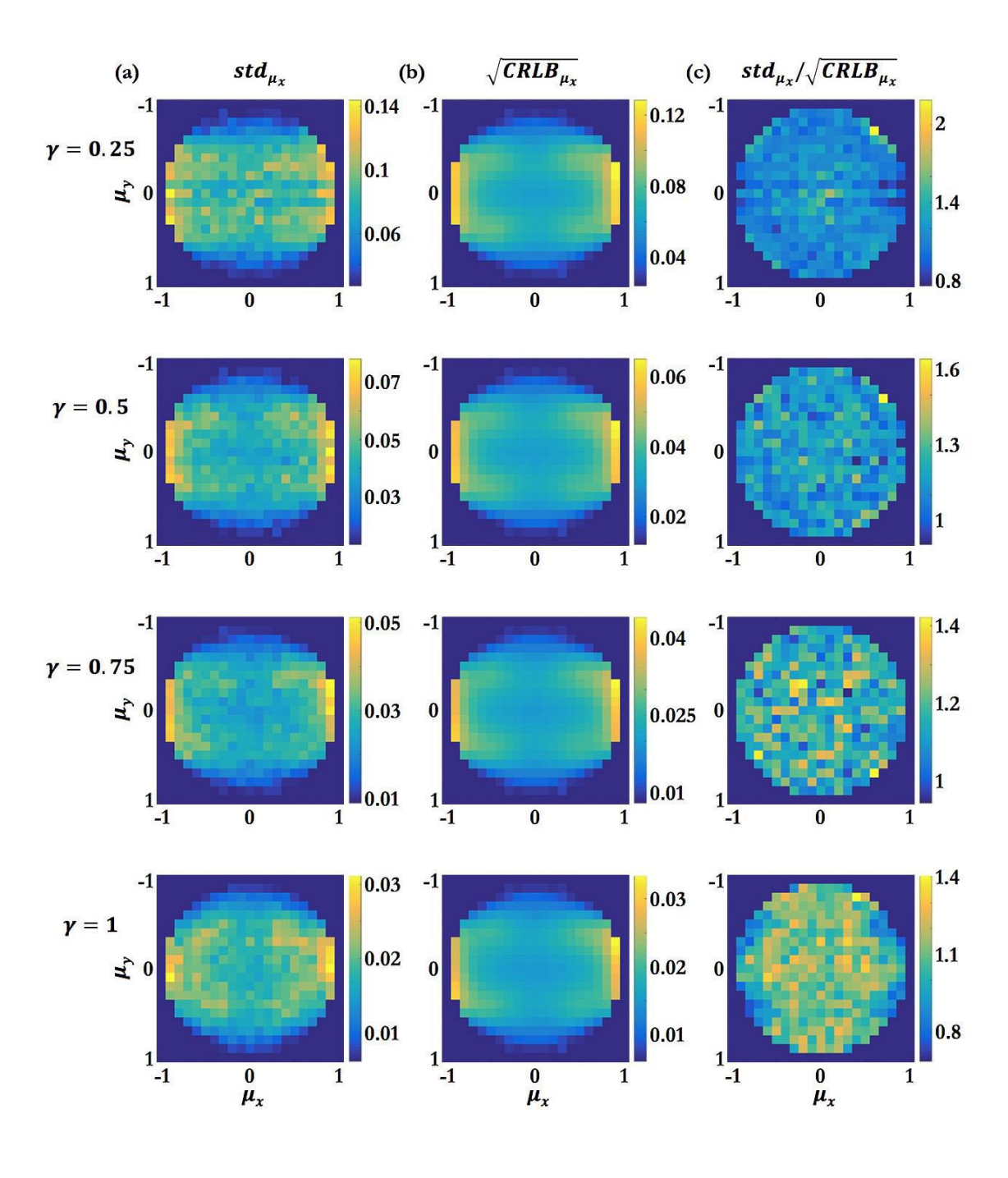
As inspiration, we examine the orientation-sensing strategy of the bisected²⁰ and quadrated²¹ phase masks and note that these phase masks split the standard PSF into 2 or 4 spots, respectively, in order to measure molecular orientation. To maximize signal-to-noise ratio under shot noise-limited conditions, which scales as \sqrt{N} , where N is the number of photons detected, we wish to minimize the number of spots within our PSF while maintaining sufficient degrees of freedom to measure all second moments of M. Due to the definition of μ (Eqn. (1)), we note that $\langle \mu_x(t)^2 \rangle + \langle \mu_y(t)^2 \rangle + \langle \mu_z(t)^2 \rangle = 1$. Therefore, we desire a PSF that can measure 5 orientational and 1 brightness degree of freedom – thus, a 6-spot PSF. If we utilize an imaging system with two polarization channels, then a PSF containing 3 spots, or the Tri-spot PSF, will suffice.

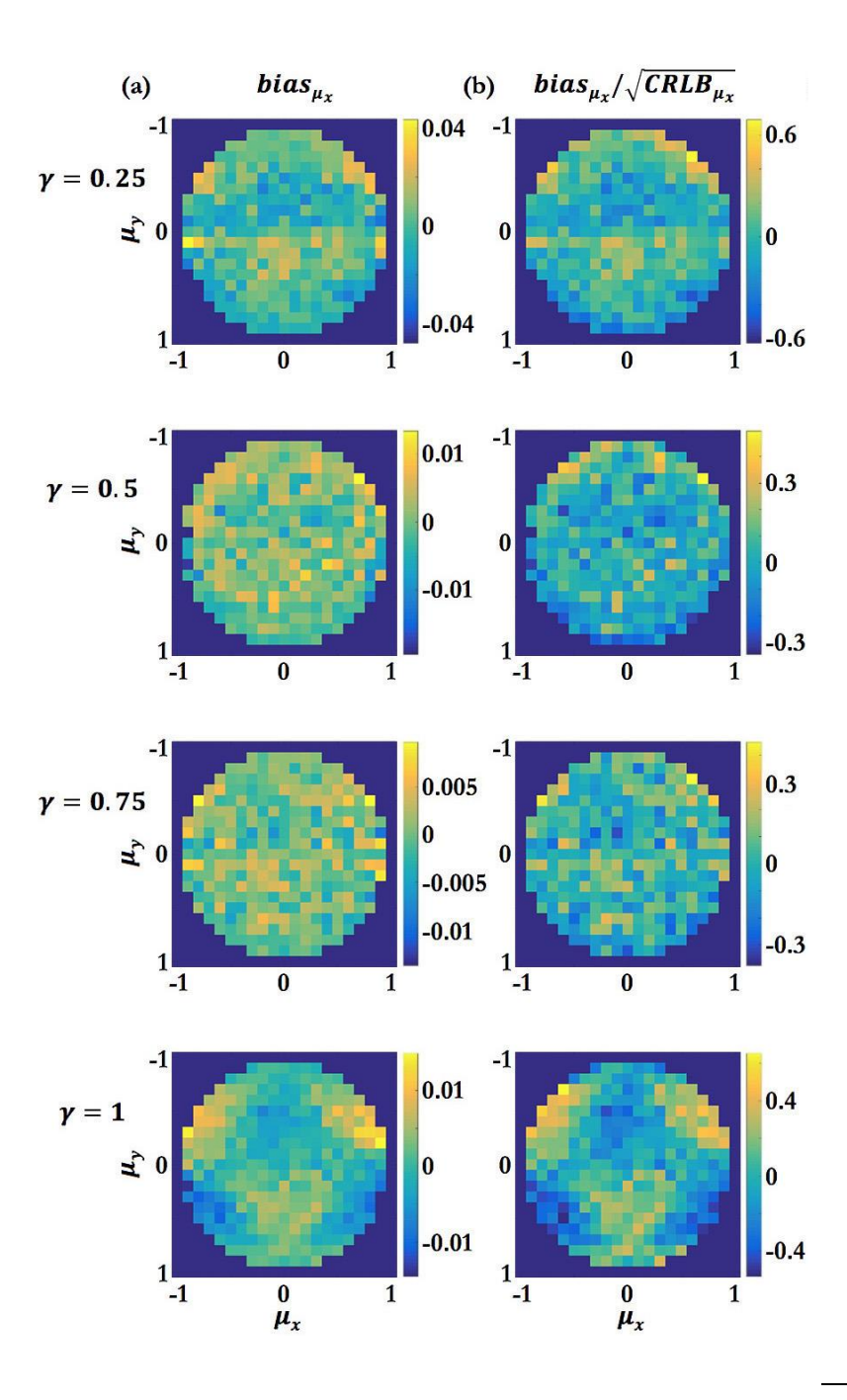
Utilizing an existing vectorial diffraction model¹³, we tested various phase mask designs that split the back focal plane, or pupil plane, of the microscope into three partitions. We placed a linear phase ramp within each partition to create three off-center, focused spots in the imaging plane. The arrangement of spots was designed to be a triangle to avoid assignment ambiguity resulting from the absence of one spot. The partition shapes within the Tri-spot phase mask were designed to avoid orientation measurement degeneracies like the one shown in Figure 1.

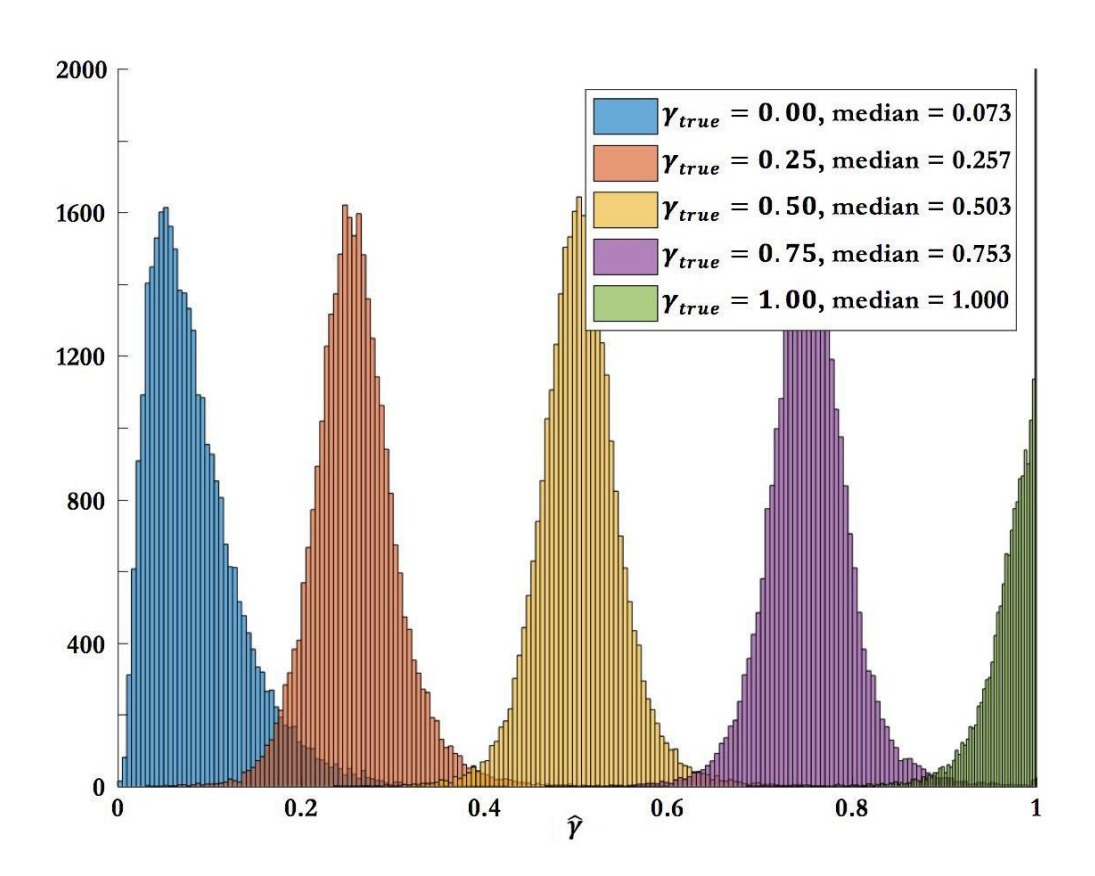


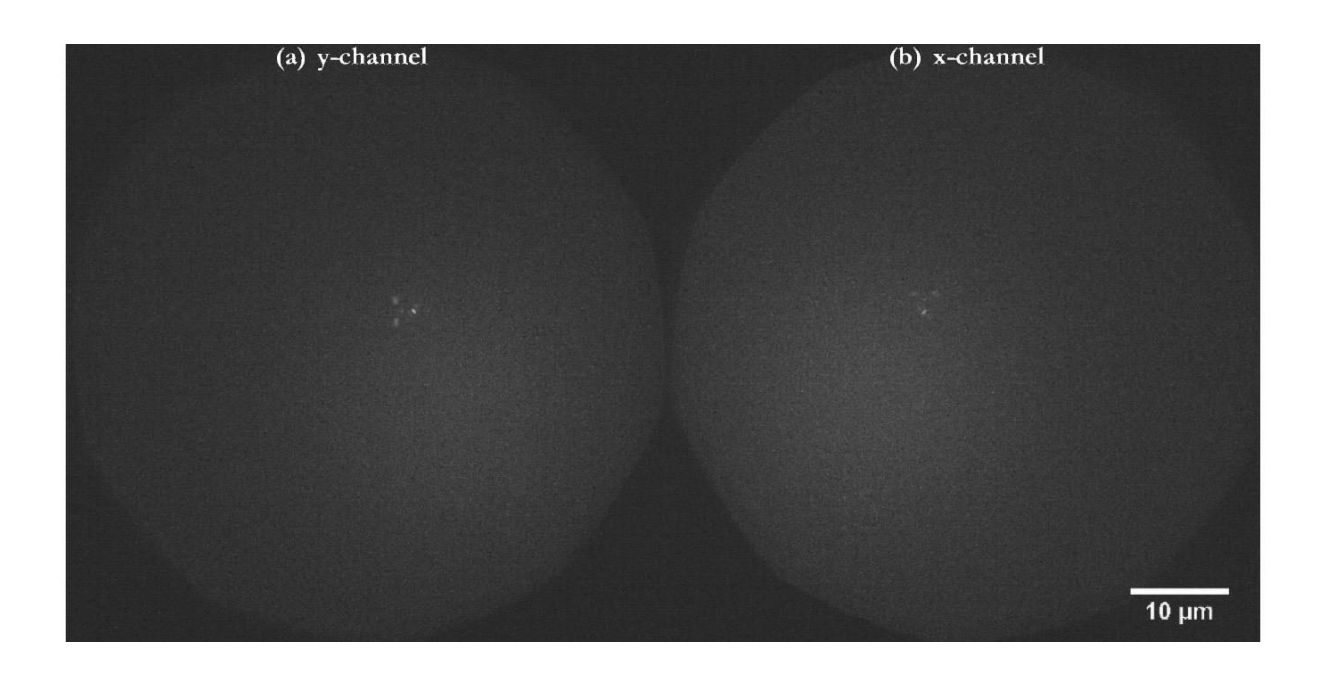


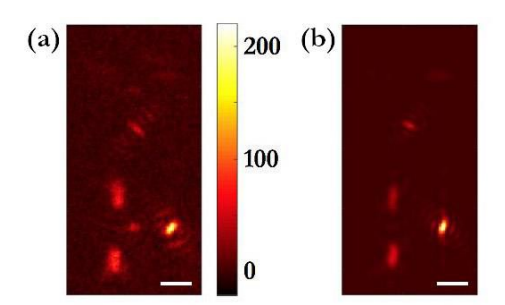


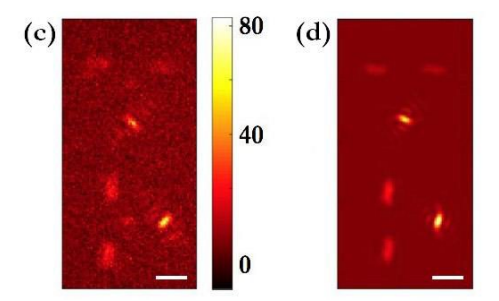


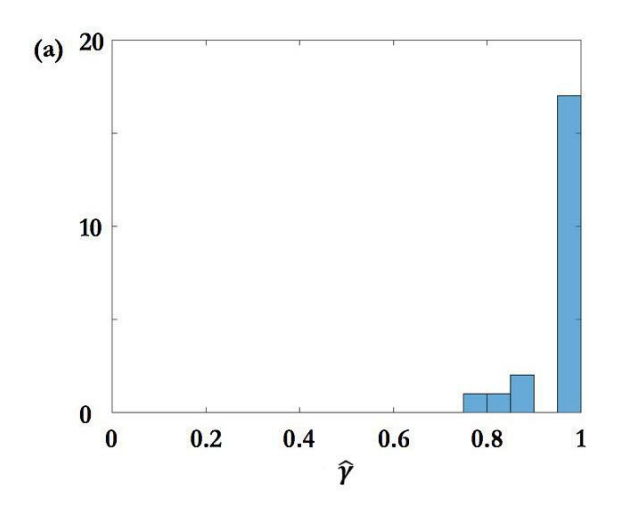


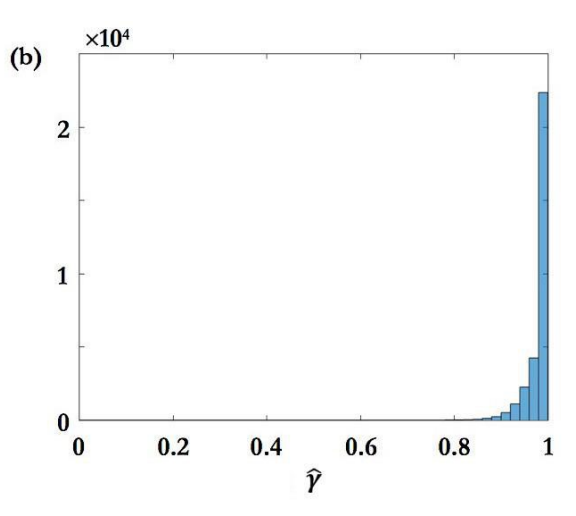












- [6] Corrie, J. E., Brandmeier, B. D., Ferguson, R. E., Trentham, D. R., Kendrick-Jones, J., Hopkins, S. C., van der Heide, U. A., Goldman, Y. E., Sabido-David, C., Dale, R. E., Criddle, S. and Irving, M., "Dynamic measurement of myosin light-chain-domain tilt and twist in muscle contraction.," Nature **400**(6743), 425–430 (1999).
- [7] Peterman, E. J. G., Sosa, H., Goldstein, L. S. B. and Moerner, W. E., "Polarized Fluorescence Microscopy of Individual and Many Kinesin Motors Bound to Axonemal Microtubules," Biophys. J. **81**(5), 2851–2863 (2001).
- [8] Sosa, H., Peterman, E. J. G., Moerner, W. E. and Goldstein, L. S. B., "ADP-induced rocking of the kinesin motor domain revealed by single-molecule fluorescence polarization microscopy," Nat. Struct. Biol. 8(6), 540–544 (2001).
- [9] Forkey, J. N., Quinlan, M. E. and Goldman, Y. E., "Protein structural dynamics by single-molecule fluorescence polarization.," Prog. Biophys. Mol. Biol. 74(1–2), 1–35 (2000).
- [10] Backer, A. S., Lee, M. Y. and Moerner, W. E., "Enhanced DNA imaging using super-resolution microscopy and simultaneous single-molecule orientation measurements," Optica 3(6), 659 (2016).
- [11] Rosenberg, S. a, Quinlan, M. E., Forkey, J. N. and Goldman, Y. E., "Rotational motions of macro-molecules by single-molecule fluorescence microscopy.," Acc. Chem. Res. **38**(7), 583–593 (2005).
- [12] Lieb, M. A., Zavislan, J. M. and Novotny, L., "Single-molecule orientations determined by direct emission pattern imaging," J. Opt. Soc. Am. B **21**(6), 1210 (2004).
- [13] Backer, A. S. and Moerner, W. E., "Extending single-molecule microscopy using optical fourier processing.," J. Phys. Chem. B **118**(28), 8313–8329 (2014).
- [14] Pavani, S. R. P., Thompson, M. A., Biteen, J. S., Lord, S. J., Liu, N., Twieg, R. J., Piestun, R. and Moerner, W. E., "Three-dimensional, single-molecule fluorescence imaging beyond the diffraction limit by using a double-helix point spread function," Proc. Natl. Acad. Sci. **106**(9), 2995–2999 (2009).
- [15] Lew, M. D., Lee, S. F., Badieirostami, M. and Moerner, W. E., "Corkscrew point spread function for far-field three-dimensional nanoscale localization of pointlike objects.," Opt. Lett. **36**(2), 202–204 (2011).
- [16] Jia, S., Vaughan, J. C. and Zhuang, X., "Isotropic three-dimensional super-resolution imaging with a self-bending point spread function," Nat. Photonics **8**(4), 302–306 (2014).
- [17] Shechtman, Y., Weiss, L. E., Backer, A. S., Sahl, S. J. and Moerner, W. E., "Precise Three-Dimensional Scan-Free Multiple-Particle Tracking over Large Axial Ranges with Tetrapod Point Spread Functions," Nano Lett. **15**(6), 4194–4199 (2015).
- [18] von Diezmann, A., Shechtman, Y. and Moerner, W. E., "Three-Dimensional Localization of Single Molecules for Super-Resolution Imaging and Single-Particle Tracking," Chem. Rev. **117**(11), 7244–7275 (2017).
- [19] Shechtman, Y., Weiss, L. E., Backer, A. S., Lee, M. Y. and Moerner, W. E., "Multicolour localization microscopy by point-spread-function engineering," Nat. Photonics **10**(9), 590–594 (2016).
- [20] Backer, A. S., Backlund, M. P., von Diezmann, A. R., Sahl, S. J. and Moerner, W. E., "A bisected pupil for studying single-molecule orientational dynamics and its application to three-dimensional super-resolution microscopy," Appl. Phys. Lett. **104**(19), 193701 (2014).
- [21] Backer, A. S., Backlund, M. P., Lew, M. D. and Moerner, W. E., "Single-molecule orientation measurements with a quadrated pupil," Opt. Lett. **38**(9), 1521 (2013).
- [22] Backlund, M. P., Lew, M. D., Backer, A. S., Sahl, S. J., Grover, G., Agrawal, A., Piestun, R. and Moerner, W. E., "Simultaneous, accurate measurement of the 3D position and orientation of single molecules.," Proc. Natl. Acad. Sci. U. S. A. 109(47), 19087–19092 (2012).
- [23] Kay, S. M., [Fundamentals of statistical signal processing], Prentice Hall, Englewood Cliffs, N.J. (1993).
- [24] Shechtman, Y., Sahl, S. J., Backer, A. S. and Moerner, W. E., "Optimal Point Spread Function Design for 3D Imaging," Phys. Rev. Lett. **113**(13), 133902 (2014).